

Article

Hydration Phenomena of Functionalized Carbon Nanotubes (CNT)/Cement Composites

Bhuvaneshwari Balasubramaniam ^{1,*}, Kunal Mondal ^{2,*}, Karunya Ramasamy ³,
Gadyam S. Palani ^{4,*} and Nagesh R. Iyer ⁵

¹ Department of Chemical Engineering, Indian Institute of Technology, Kanpur 208016, Uttar Pradesh, India

² Department of Chemical & Biomolecular Engineering, NC State University, Campus Box 7905, Raleigh, NC 27695-7905, USA

³ Department of Mechanical Engineering, Indian Institute of Technology, Chennai 600036, Tamil Nadu, India; sendmailtokaru@gmail.com

⁴ Steel Structures Laboratories, CSIR-Structural Engineering Research Centre, Chennai 600113, Tamil Nadu, India

⁵ Academy of Scientific & Innovative Research (AcSIR), Chennai 600113, Tamil Nadu, India; nageshiyer@gmail.com

* Correspondence: bhuvib@iitk.ac.in (B.B.); kmondal@ncsu.edu (K.M.); pal@serc.res.in (G.S.P.); Tel.: +91-8015536711 (B.B.); +1-919-260-9449 (K.M.); +91-9444945902 (G.S.P.)

Academic Editor: Sushanta Ghoshal

Received: 28 August 2017; Accepted: 16 October 2017; Published: 19 October 2017

Abstract: The exciting features of carbon nanotubes (CNTs), such as high elastic modulus, high thermal and electrical conductivities, robustness, and nanoscopic surface properties make them attractive candidates for the cement industry. They have the potential to significantly enhance engineering properties. CNTs play an important and critical role as nano-anchors in concrete, which enhance the strength by bridging pores in the composite matrix, thereby ensuring robust mechanical strength. The diameter, dispersion, aspect ratio, and interfacial surface interaction of CNTs affect the physical and mechanical properties of concrete, if due care is not taken. In this paper, the usable amount of CNT is scaled down considerably from 0.5% to 0.025% by weight of the cement and the fluctuation caused by these phenomena is assessed. It is observed that the properties and exact quantities of incorporated CNTs influence the hydration and consistency of the composites. In order to address these issues, the surface functionalization of CNTs and rheological studies of the composites are performed. The hydration products and functional groups are carefully optimized and characterized by using X-ray diffraction (XRD), Fourier transform infrared spectroscopy (FTIR), scanning electron microscopy (SEM), and a Zeta potential analyzer. For Mixes 6 and 7, the compressive and tensile strength of CNTs incorporated in mortar specimens caused 77% and 48% increases in split tensile strength, respectively, and 17% and 35% increases in compressive strength, respectively, after 28 days of curing and compared with the control Mix.

Keywords: carbon nanotubes (CNT); cement; cement composites; hydration products; surface functionalization; Micro Structural Characterization; compressive and tensile strengths

1. Introduction

The first awareness about carbon nanotubes (CNTs) was brought to the scientific community in 1991 by Iijima [1], and, two years later, a single-wall CNT was discovered [2]. Although the last decade has witnessed the development of nanotechnology in various fields such as space, energy, health, and environment, the nanomaterial industries based on 0D (zero dimension), 1D, and 3D materials are still in their infant stage and only few have been studied [3–5]. CNTs were considered

a new and outstanding material with great potential applications in composites technology [6,7]. CNTs possess covalent sp^2 bonds between individual carbon atoms and an ultra-high mechanical strength with Young's modulus of 1.2 TPa [8]. It is important to note that the tensile strength of CNTs [9] is nearly 100 times higher than that of steel [10]. Based on their indices (n, m) CNTs are classified as either metallic, semi-conducting, or a small-gap semi-conductor, mainly depending on the diameter and chirality. The carbon atoms in CNTs are arranged in a periodic hexagonal manner with a cylindrical shell shape and are classified as single-walled nanotubes (SWNTs) or multi-walled nanotubes (MWNTs) [11].

Recently, Mehta's group published a review on the consequences of CNTs on the properties of cement mortars, which evidently shows that numerous attempts have been made by various authors towards enhancing the compressive strength, flexural strength, microstructure, Young's modulus, and porosity of cement–CNT composites [12]. The effect of the addition of CNTs to cement-based materials was also investigated to effectively change their brittleness and develop materials with superlative mechanical properties [13–17]. Besides all the benefits, certain issues such as poor dispersion, high entanglement with matrix, agglomeration, interfacial strain transfer, lack of functional sites, etc., limit the global use of CNTs. This remains the challenge for high performance composite applications [18–21]. Many studies in the recent past have demonstrated the compatible dispersion, surface functionalization, and changes in surface energy of the nanotube with the goal of tapping the tremendous potential of CNTs as a reinforcing material for high performance cementitious composites [11,22–25].

As reported in previous studies, it is described that although surface treatment of CNTs via chemical modifications to create the carboxyl surface increases the mechanical strength, some studies have proved a negative impact on the strength properties [26]. This is mainly due to the chemicals used for functionalization, which degrade the mechanical properties of CNTs. This also creates many uncertainties and uncontrolled variables when mixed with concrete. Also, various polymers or water are used for the dispersion of CNTs with the help of ultrasonication [27–34]. A detailed report on the effect of the functionalization of CNTs for the use of concrete/mortar by various research groups was discussed by Krause et al. [35]. It is also reported that chemical treatments are environmentally unfriendly, which can harm the hydration products resulting in reduced mechanical strength. Hence, polycarboxylic (PC) based dispersing and functionalizing agents are employed in the present study for creating functionalized CNTs (f-CNTs). Reports available on the use of PC-based functionalizing agents to create f-CNTs for enhancing the mechanical properties of mortar/concrete are very scanty. One of the important factors to be noted in choosing PC is its high compatibility with cementitious matrices. Hence, it is expected that it will not harm the environment of the mortar/concrete during strength development. Proper dispersion and mixing methods are the prime parameters responsible for well-coordinated contact between the hydration products and MWCNTs. At this time, chemical and physical modifications are the two important techniques largely used for CNT dispersion [36]. It is proven that the use of polycarboxylic-based superplasticizer as a functionalizing agent for CNT/cement composites enhances the mechanical strength through uniform dispersion with negligible agglomeration. Improvement in the flexural strength has also been demonstrated [37].

In this study, an efficient strategy is proposed to improve the mechanical properties of the CNT-cement nanocomposites using functionalized CNTs during hydration. This has also been compared with non-functionalized CNTs. The microstructural investigation of the nanocomposites reveals that CNT helps in filling up micro/nano pores between the calcium silicate hydrate (CSH) and ettringite during the process of hydration, which is in agreement with previous studies [34,38–42]. It is also envisaged that providing an adequate force between CNTs and the composite matrix is essential, which provides information for better understanding of the load transfer mechanisms in composite materials. The effect of highly dispersed functionalized CNTs on the mechanical properties of cement mortar composites is also demonstrated in this study.

2. Experimental

2.1. Materials

MWNTs with a diameter of 15 ± 5 nm and length of 1–5 microns were employed in the investigation, and were procured from M/s NanoShell, USA. In essence, the structure of MWNTs is an array of multiple concentric nanotubes precisely nested within one another. PC based superplasticizer was chosen based on its comparable compatibility with the cement matrix and the active non-polar groups within the molecule. Ordinary Portland Cement (OPC) 53 grade and fine aggregates passing through 2.36 microns, conforming to the requirements of IS:12269 and IS:383, were used as binding and filler materials. Potable water was used for mixing throughout the study.

2.2. Surface Functionalization of CNTs with PC

Proper functionalization methods are required to achieve absolute efficiency of cement–CNT composites. In this study, the ultrasonication method was chosen for surface functionalization of CNTs with PC superplasticizer, a compatible polymer. During ultrasonication, particles in a solution are agitated to form a colloidal dispersion due to the action of ultrasound energy. The sonicator used in this study was procured from M/s Ultrasonics, USA, and has an adjustable amplitude ranging from 20% to 60% and a power of 700 W at 20 Hz. Before starting the sonication, the PC was diluted to reduce its viscosity according to the water/cement (W/C) ratio, as presented in Table 1. Thereafter, the required amounts of diluted PC and CNTs were taken in a beaker, dispersed via hand stirring, and kept under ultrasonication for 2 h. A probe with a diameter of 1.1 cm and length of 7 cm was used for dispersion of the colloidal nanocomposites. The cut-off ratio to control the temperature was kept at 2 min with a break in each 20 min agitation. An ice-bath was used to control the agglomeration of nanotubes due to heat dissipation during the operation, which also maintained the solvent viscosity. All these parameters were chosen based on the optimization studies conducted at various stages.

2.3. Characterization

In order to confirm the response surface created on the CNTs through functionalization, zeta or surface potential measurements were carried out. In the case of functionalized CNTs (f-CNTs), measurement was carried out after the functionalization, whereas for non-functionalized CNTs (nf-CNTs), zeta potential was measured after sonicating the CNTs in an aqueous medium only for 2 min. The zeta potential was calculated using Malvern Instruments Ltd., Malvern, UK, according to the Henry equation by using the Smoluchowski approximation. A Transmission Electron Microscopy (TEM) study was conducted to ensure the non-agglomeration of chelated and surface-activated f-CNTs. An accelerating voltage of 300 kV, with the aid of a Hitachi H-9500N instrument (Hitachi Ltd., Tokyo, Japan), was used for TEM study. X-ray diffraction (XRD) (Bruker Group GmbH, Karlsruhe, Germany), Fourier transform infrared spectroscopy (FT-IR), and scanning electron microscopy (SEM) were collected after 1 day, 7 days, and 28 days of hydration.

Powder X-ray diffraction data of prepared materials were collected on a Bruker D2 Phaser Desktop X-Ray Diffractometer (30 kV and 10 mA) equipped with Ni-filtered Cu K α radiation ($\lambda = 1.542$ Å). Data were captured over the range of (2 θ) 5 to 70° with a step size of 0.0017 and a scan rate of 7°/min. FT-IR (Nicolet 6700) (ThermoFisher Scientific, Waltham, MA, USA) studies were conducted in the frequency region of 4000–400 cm^{−1} in the transmittance mode. SEM (TESCAN, Brno, Ceska Republika) studies were performed to assess the morphological changes of hydration products.

2.4. Mechanical Characterization of Cement CNT Mortars

A mechanical strength characterization of f-CNTs and nf-CNTs incorporated into cement mortar specimens was carried out. Here, Mix 3 to Mix 5 and Mix 6 to Mix 8 represent the cement mortars with non-functionalized and functionalized CNTs respectively. The mixes used for casting the mortar

specimens are presented in Table 1. Control specimens were also cast for comparison purposes. The cement to sand ratio was kept at 1:3. The water to cement ratio was arrived at based on the consistency and setting time carried out for the corresponding mixes as per IS 4031. The CNT content was arrived at by weight of cement used. Special consideration was given during the mixing of cement with CNTs. The dimensions of the mortar cube specimens were 50 mm × 50 mm × 50 mm, and cylinder specimens were 75 mm × 150 mm, for evaluating the compressive and split tensile strength after curing for 3, 7, 14, 28, 45, and 56 days. The tests were conducted using a 2000 kN capacity universal testing machine (UTM). During split tensile measurements, plywood strips of suitable thickness were placed between the specimen and loading plates of the UTM to avoid high compressive stress at the points of application of load. The rate of loading applied for the compressive and split tensile strength tests was 0.6 kN/s and 1.2 kN/s, respectively. Each testing involved at least six different specimens at the respective days.

Table 1. Mix Details.

| Mix ID | Mix Details | Water/Cement (W/C) Ratio | % of Polycarboxylic Superplasticiser with Respect to the W/C |
|--------|---|--------------------------|--|
| Mix-1 | Neat cement | 0.40 | None |
| Mix-2 | Neat cement | 0.28 | 0.5 |
| Mix-3 | Cement + 0.025% Carbon Nanotubes (CNTs) | 0.56 | None |
| Mix-4 | Cement + 0.05% CNTs | 0.68 | None |
| Mix-5 | Cement + 0.5% CNTs | 0.80 | None |
| Mix-6 | Cement + 0.025% CNTs | 0.35 | 0.5 |
| Mix-7 | Cement + 0.05% CNTs | 0.40 | 0.5 |
| Mix-8 | Cement + 0.5% CNTs | 0.45 | 0.5 |

3. Results and Discussion

3.1. Morphological Studies

TEM images of f-CNT and the Zeta potential distributions of f-CNTs and nf-CNTs are shown in Figure 1a,b, respectively. The typical electro-kinetic potential obtained for f-CNTs present in Mix 6 was −14.9 mV, as shown in Figure 1b, whereas for nf-CNTs present in Mixes 3, 4, and 5, it was −6.33 mV, −5.77 mV, and −5.38 mV, respectively. Enhancement of surface potential is an indication of possible attachment of CNTs with active non-polar groups present in the PC molecule, which effectively chelates or disperses CNTs [11].

In the case of nf-CNTs, surface potential is reduced by increasing CNT content, which is indicative of the agglomeration of nanotube bundles. Further, no sedimentation is noticed after functionalization of f-CNTs as present in Mix 6 compared to other f-CNT mixes. Hence, the zeta potential value for Mix 6 is taken as reference for indicating the surface potential enhancement of f-CNTs as shown in Figure 1b. The TEM image of the same mix is shown in Figure 1a, which is evidence for non-agglomerated and highly dispersed f-CNTs. For the other f-CNT mixes, little agglomeration is noticed from TEM study. It is observed from the studies that effective functionalization and surface enhancements on CNTs are possible through the selection of a suitable chelating agent and adopting optimized sonication methods. The typical sketch of possible interaction of f-CNTs with water and PC is shown using schematics in Figure 2a,b.

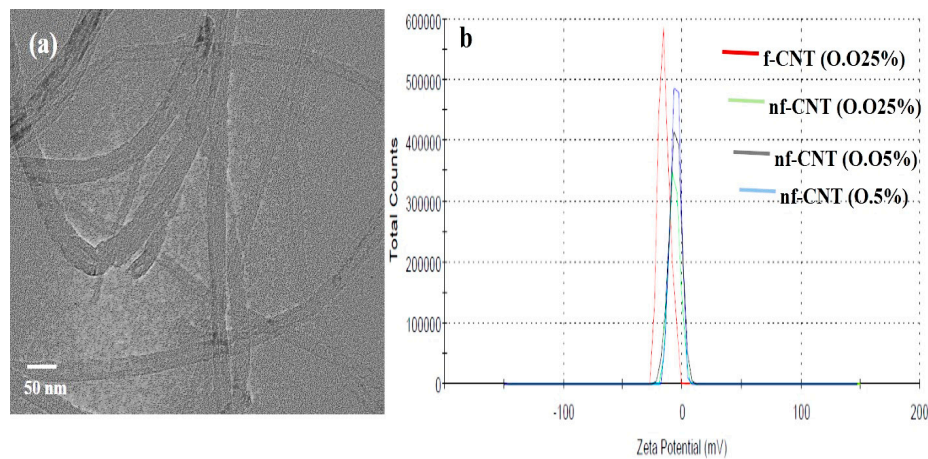


Figure 1. (a) Transmission electron microscopy (TEM) image of functionalized carbon nanotube (f-CNT); and (b) Zeta potential distribution curve of f-CNTs and non-functionalized CNTs (nf-CNTs).

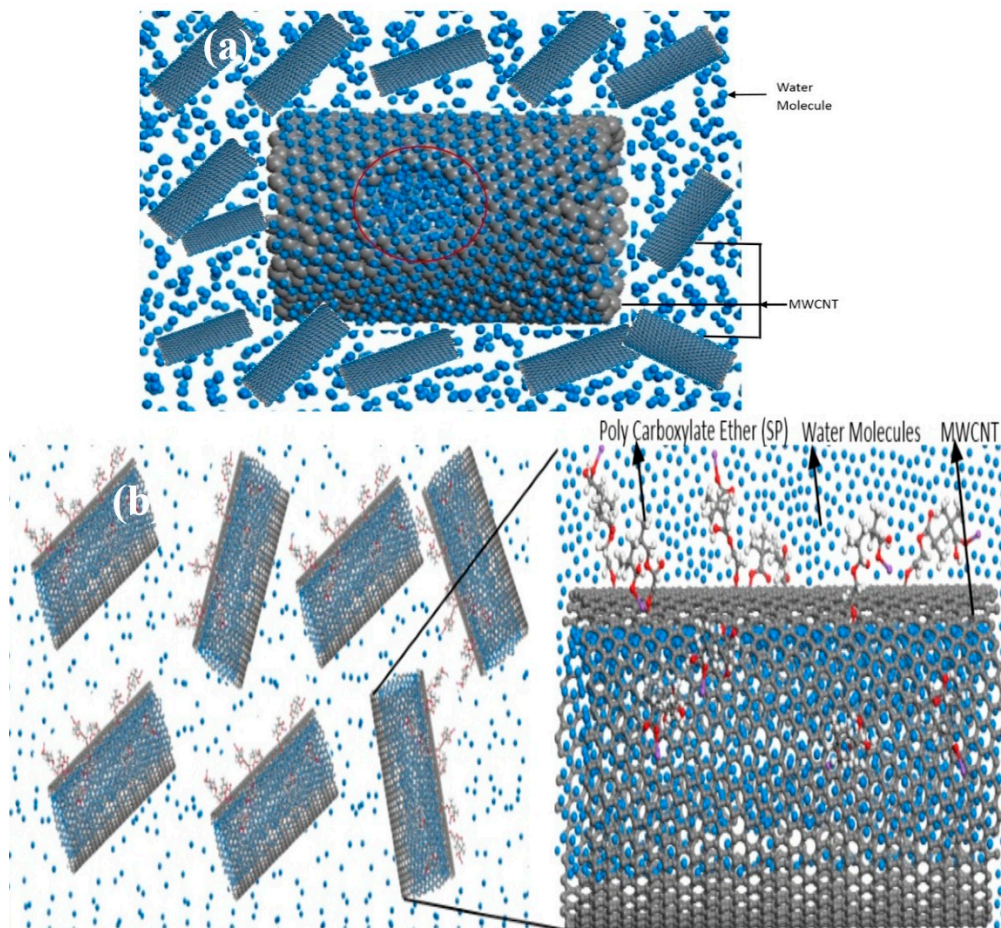


Figure 2. Schematic representation of (a) dispersion of CNT in water; and (b) surface activated f-CNTs.

The hydration products formed during the hydration at 24 h, the 7th day, and the 28th day for all mixes were evaluated using XRD analysis (Figure 3). Identification of XRD patterns of hydration products were carried out with the International Crystal Diffraction Database (ICDD) software. XRD analysis of the hydration process clearly depicts the formation of hydration products at

various intervals. Due to the limitation on identification of amorphous substances through XRD, it is not possible to detect the calcium-silicate-hydrate gel (C-S-H), a main hydration product of cement. However, crystalline hydration products of cement can be analyzed. In XRD spectra, hydration products such as ettringite (e), portlandite (P), tricalcium silicate or alite (a), dicalcium silicate or belite (b), and tetracalcium aluminoferrate (C4AF) are denoted.

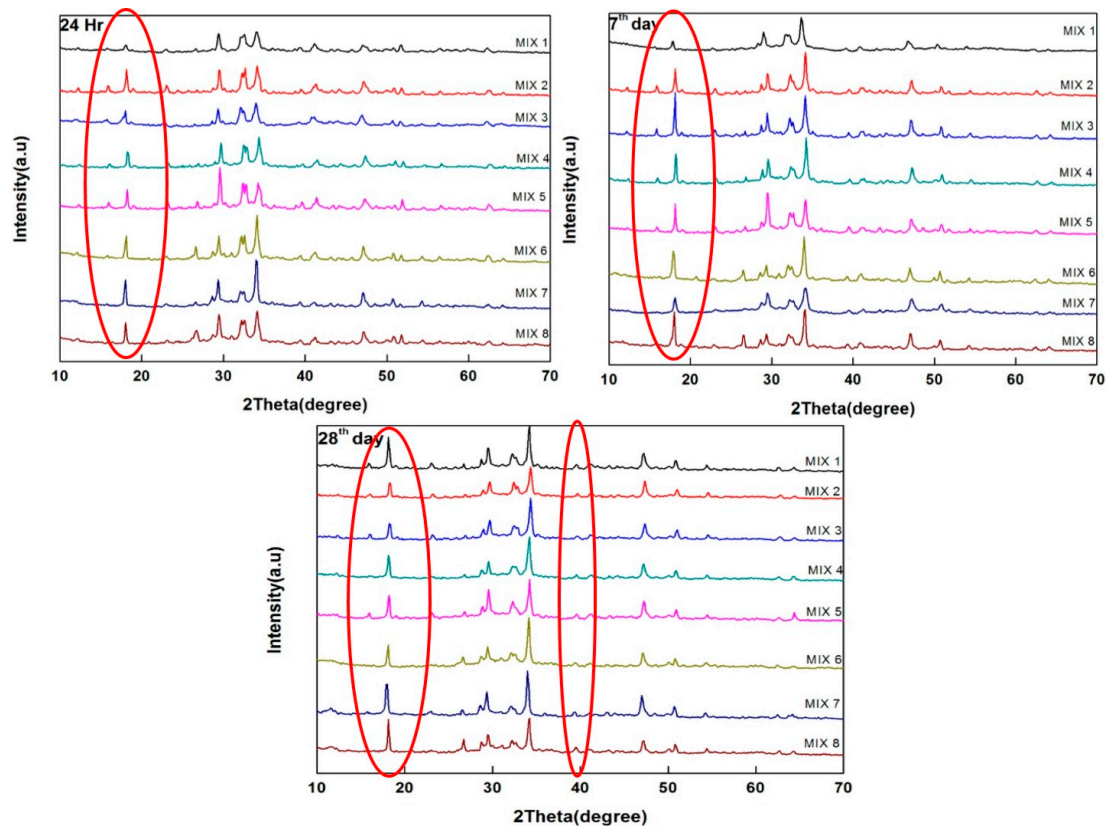


Figure 3. X-ray diffraction (XRD) spectra of all Mixes during various hydration intervals.

It is observed that in Mixes 6 to 8 at 24 h, ettringite ($C_6AS_3H_{32}$) and portlandite ($Ca(OH)_2$) have formed as indicated at 2 theta of 14 and 28, respectively. At the same time, it can be inferred that on the 7th day of hydration, a decrease in the peak intensity for Mixes 6 and 7 occurred. On the 28th day of hydration, it can be observed that the peak intensities attributed to the alite and belite phases decrease, which indicate the conversion of unhydrated phases into hydrated phases [43]. Also in Mixes 6 and 7 (on the 28th day), the appearance of a new peak at 2 theta 39 indicates aluminosilicate formation. A well refined and highly intense portlandite peak at 2 theta 18 for Mixes 6 and 7 (on the 28th day) indicate the effective hydration of the respective mixes [43]. They indicate the enhanced reaction of Ca^{+} ions and $Ca(OH)_2$, resulting in high C-S-H gel formation, which obviously reduces the porosity that occurred during hydration. The above characteristics are absent in Mixes 3 to 5, which may be due to the agglomeration effect of nf-CNT during the course of hydration, which hindered the hydration process. It is also evident from the XRD spectra of Mix 8 that, due to the higher CNT content, the growth of hydration products was affected and hence C-S-H conversion was reduced. This happened mainly due to the bundling effect of CNTs, which hindered the hydration product formation. The bundling effect is discussed in detail with the support of SEM analysis. Hence, XRD analysis of the cement–CNT nanocomposites showed that the addition of properly functionalized CNTs has a positive impact on the process of hydration, which directly influences mechanical properties.

By considering the limitations of XRD on the detection of main hydration product C-S-H, FT-IR analysis was conducted for analyzing the hydration products; this is shown in Figure 4. The bands at 1000 cm^{-1} , 3643 cm^{-1} , 1110 cm^{-1} , and 560 cm^{-1} for all the mixes confirmed functional groups like C–O stretch, O–H stretch, Si–O, and poly sulphides ($-\text{SO}_3^{2-}$). The band at 970 cm^{-1} denotes C-S-H gel [43,44]. For the nanocomposite mixes, the band intensity of the –OH group is lower at 3643 cm^{-1} . The decrease in intensity of the band at 3643 cm^{-1} for Mixes 6 and 7 in all three days of selected hydrations indicates the possible interaction of –COOH or C–OH present on CNTs and portlandite.

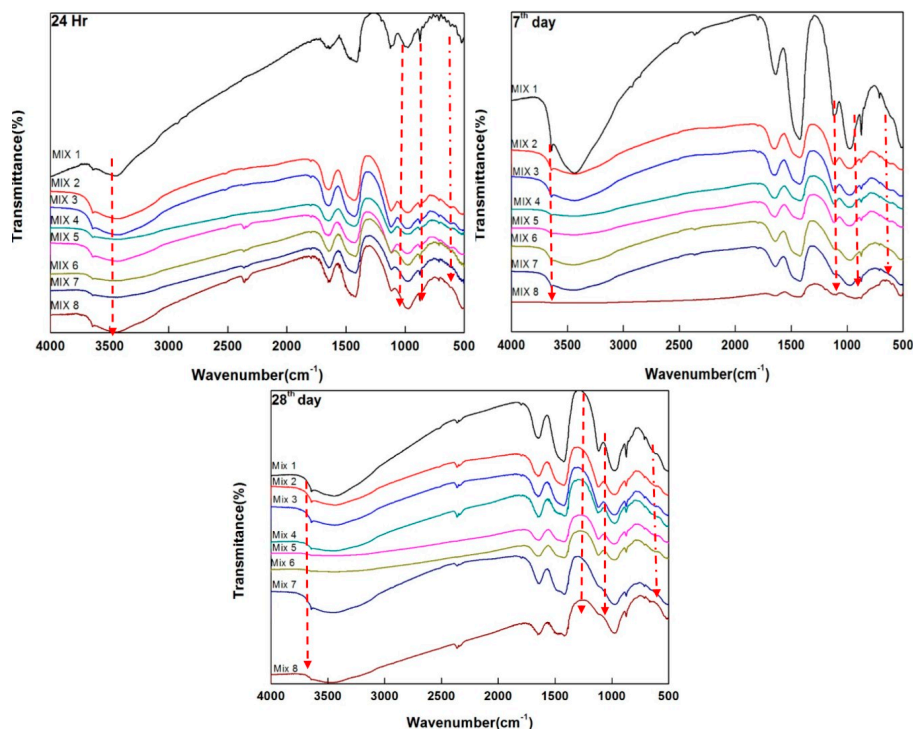


Figure 4. FT-IR spectra of hydration of all Mixes during various hydration intervals.

SEM images showing the hydration of cement–CNT nanocomposites at different time intervals such as 5 h, 24 h, day 7, and day 28 are shown in Figures 5–8. From SEM images, the following are observed.

- For Mix 1 at 5 h, pores slowly started appearing due to the evaporable water during the process of setting, as indicated by the circle. This pore formation was rapid at 24 h, as indicated in Figure 5.
- By observing the morphology of Mix 5 at 5 h and 24 h, it can be inferred from the highlighted circles that the bundles of CNTs were patched at one point, which clearly exhibits the agglomeration behavior of the non-functionalized CNTs. This is due to the poor bonding of CNTs with cement grains, which resulted in improper dispersion. The same behavior appeared up until the 28th day of hydration.
- For Mix 7 at 5 h, it can be observed (highlighted circle) that the bridge-like formation of f-CNTs with hydration products of composites filled the thermal crack that occurred during the setting process. Further, it can be observed in the highlighted circle that a nested formation of cage-like structure occurred at 24 h of hydration in the same mix. This is evidence for the proper dispersion and chelation of CNTs, when functionalized with superplasticizer.
- Further, while comparing Mixes 5 and 7, it can be observed as indicated by the highlighted circles that, in the former case, bundles of CNTs appeared in agglomerated form due to the lack of functionalization. However, in the latter case, a well-co-ordinated and uniformly dispersed

f-CNTs-hydration matrix is observed. This proves the effective functionalization of CNTs during cement hydration and its role as a filler and crack-bridging agent, thereby enhancing mechanical strength. Since the durability of the cement composites are largely affected by the presence of the pores or cracks formed at the early stage of hydration, it is necessary to create an in-situ filler or crack-bridging agent, which will automatically take care of the durability of the composites. The observations made in the present study also support the role of f-CNTs as in-situ filler as well as a crack-bridging agent. Hence, the durability of the above composites is taken care of.

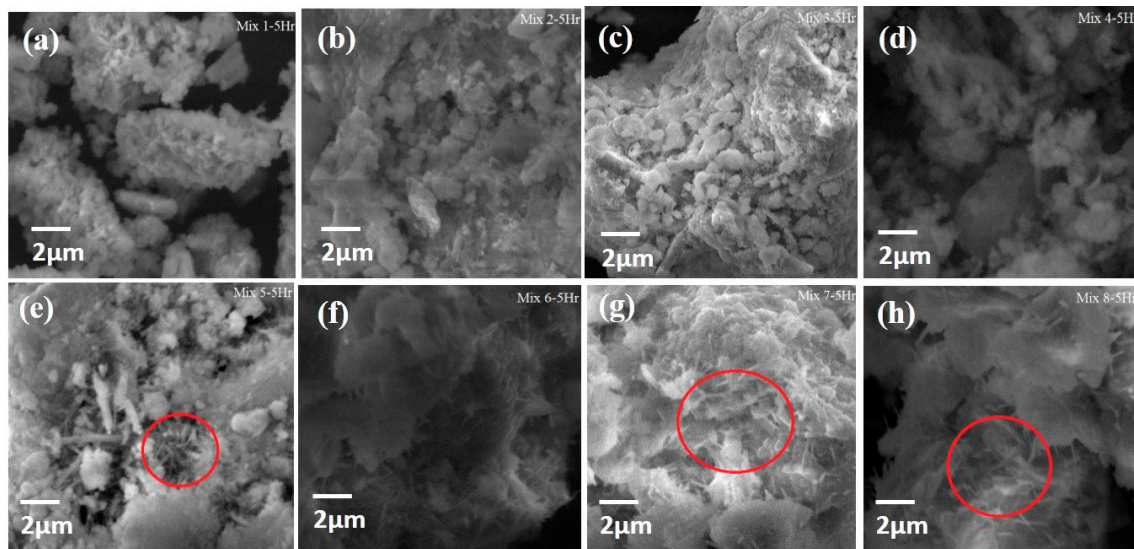


Figure 5. (a–h) SEM images represent the morphologies of Mixes 1 to 8 of hydration after 5 h.

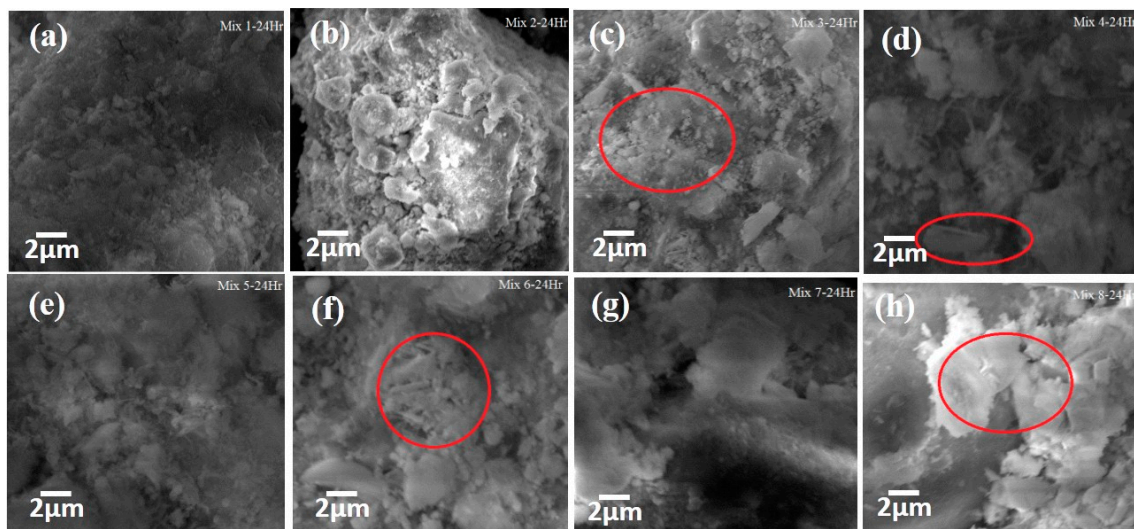


Figure 6. (a–h) SEM images represent the morphologies of Mixes 1 to 8 of hydration after 24 h.

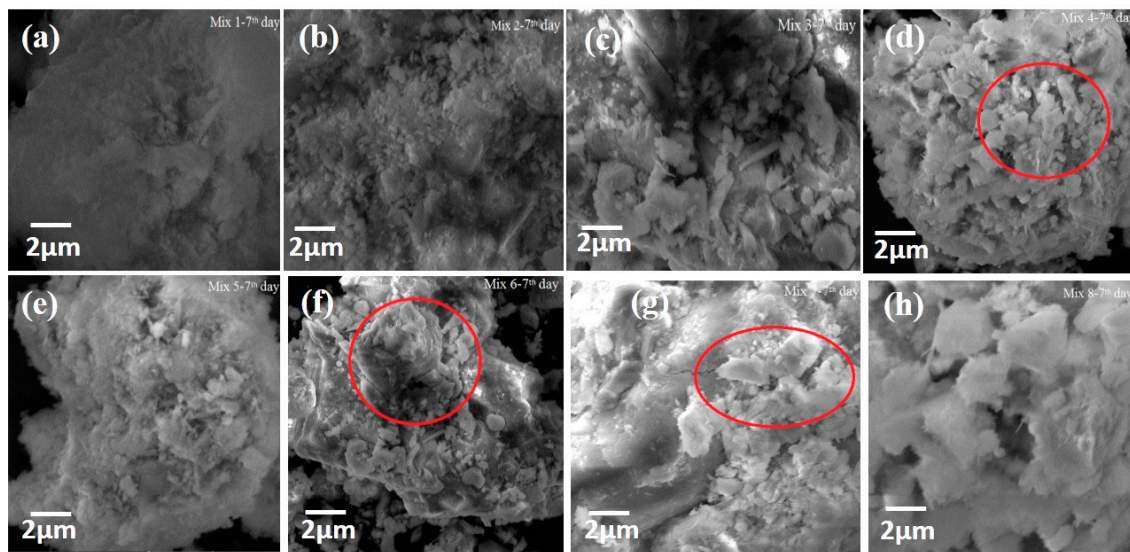


Figure 7. (a–h) SEM images represent the morphologies of Mixes 1 to 8 of hydration after the 7th day.

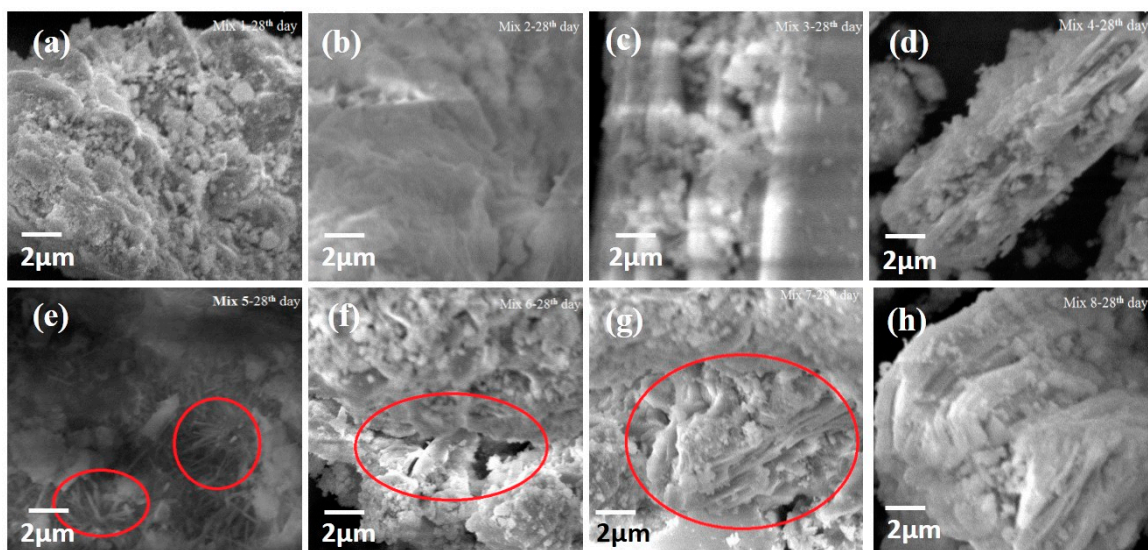


Figure 8. (a–h) SEM images represent the morphologies of Mixes 1 to 8 of hydration after the 28th day.

3.2. Mechanical Property Analysis

Results obtained from compressive and split tensile strength tests of different types of mortar specimens are shown in Figure 9a,b, respectively. From the compression tests conducted after 28 days of curing, it is observed that the compressive strength of mortar mixes with 0.025% and 0.05% f-CNTs increased by about 17% and 35%, respectively, compared with the control mix.

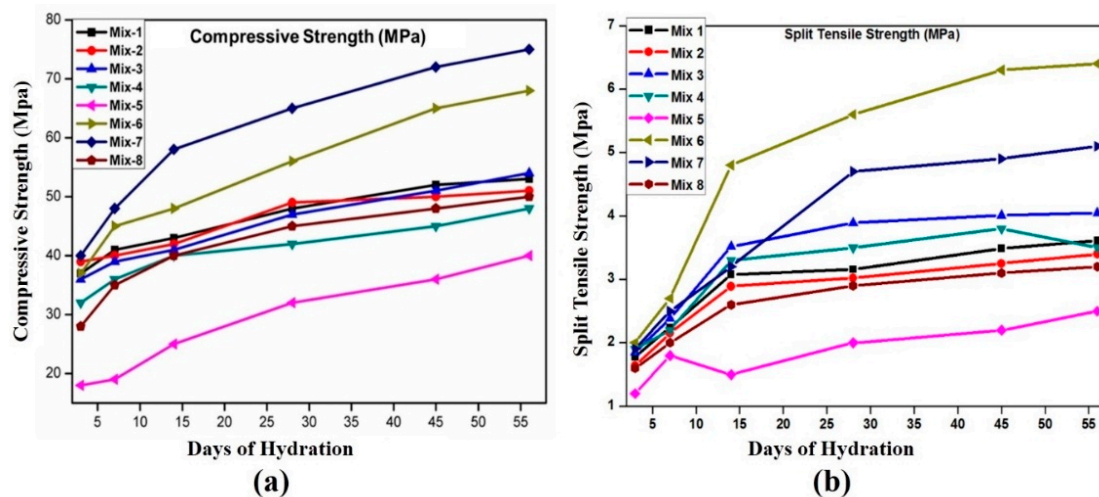


Figure 9. (a) Compressive and; (b) split tensile strengths of mortars.

In the case of split tensile strength, the mortar mixes with 0.025% and 0.05% f-CNTs showed an increase of about 77% and 48%, respectively, compared with the control mix, whereas strength is reduced for Mix 8 due to the steric hindrance effect (bundling of nanotubes due to higher concentration) of CNTs in mortar composites, which leads to a weak interface zone. As evidenced from the XRD spectra for Mixes 6 and 7, it is understood that due to the progressive formation of aluminosilicate hydrate on 28th day of hydration, an enhanced strength is noticed compared with the other mixes. SEM studies also support this claim. In general, a reduction in compressive and split tensile strength is observed for the mortars with nf-CNTs compared with mortars containing f-CNTs. A similar trend is observed for all the mortars after 56 days. Visual observations were made to identify the crack pattern of f-CNTs and nf-CNTs, and the crack patterns for the mortars were found to be dissimilar.

3.3. Failure Analysis

A SEM image of the failed specimen of Mix 6, as shown in Figure 10, emphasizes the effective reinforcement of CNTs at the interface (marked with arrows) resulting in enhanced mechanical properties compared with the control mix and mortars containing nf-CNTs.

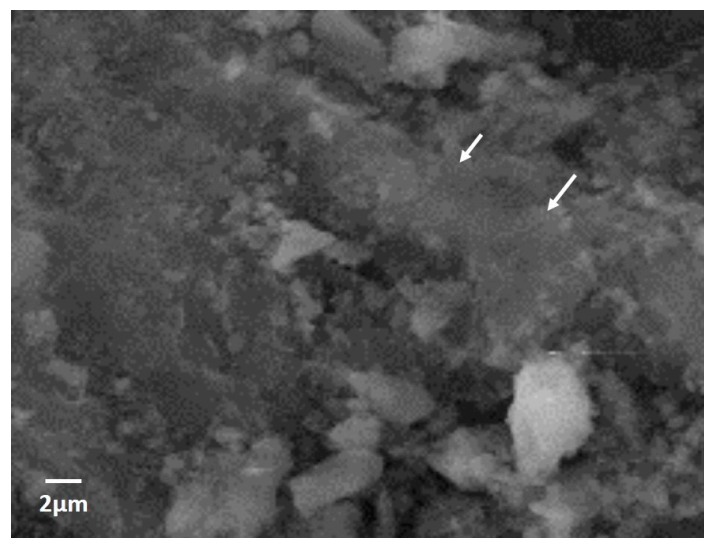


Figure 10. SEM image shows microstructure of a failed specimen (Mix 6); White arrow emphasizes the effective reinforcement of CNTs at the interface.

4. Conclusions

In summary, it is concluded that properly functionalized CNTs significantly contribute to the enhancement of the mechanical strength of cement-CNT nanocomposites. Further, functionalization of CNTs with PC is carried out by adopting an optimized sonication method. Zeta potential analysis shows that the electro-kinetic potential obtained for f-CNTs (0.025%) is -14.9 mV. TEM analysis ensured the proper dispersion of f-CNTs without agglomeration. Mechanical studies confirmed 77% and 48% increases in split tensile strength and 17% and 35% increases in compressive strength after 28 days of curing for Mixes 6 and 7, respectively, compared with the control Mix. Reductions in both compressive and split tensile strengths are noticed for Mix 8; the increased CNTs content probably created a weak interface due to a steric effect. The same trend is maintained up to day 56. SEM analysis of the failed specimen obtained after the split tensile test proves the effective reinforcement of CNTs at the mortar interface. Hence, it is concluded that enhanced mechanical properties of CNTs incorporated into cement mortar can be achieved by promoting the response surface with a suitable chelating agent and proper dispersion methods. During the process, cohesiveness of CNTs with the cement hydrate matrix needs to be ensured for effective reinforcement.

Acknowledgments: The Authors acknowledge the technical support provided by the staff members of FMCF/CSMG, CSIR-SERC, Chennai.

Author Contributions: K.R. and B.B. conceived and designed the experimental studies involving specimen preparations, casting and mechanical characterization; B.B. performed microstructural characterizations and related documentation; K.M. analyzed SEM data; G.S.P. provided guidance for the mechanical strength and microstructural studies; B.B. and K.M. wrote the paper; NRI provided overall guidance for all the activities reported in this paper

Conflicts of Interest: The authors declare no conflict of interest.

References

1. Iijima, S. Helical microtubules of graphitic carbon. *Nature* **1991**, *354*, 56–58. [[CrossRef](#)]
2. Iijima, S.; Ichihashi, T. Single-shell carbon nanotubes of 1-nm diameter. *Nature* **1993**, *363*, 603–605. [[CrossRef](#)]
3. Dowling, A.P. Development of nanotechnologies. *Mater. Today* **2004**, *7*, 30–35. [[CrossRef](#)]
4. Hullmann, A. Measuring and assessing the development of nanotechnology. *Scientometrics* **2007**, *70*, 739–758. [[CrossRef](#)]
5. Tiwari, J.N.; Tiwari, R.N.; Kim, K.S. Zero-dimensional, one-dimensional, two-dimensional and three-dimensional nanostructured materials for advanced electrochemical energy devices. *Prog. Mater. Sci.* **2012**, *57*, 724–803. [[CrossRef](#)]
6. Khan, W.; Sharma, R.; Saini, P. Carbon Nanotube-Based Polymer Composites: Synthesis, Properties and Applications. In *Carbon Nanotubes-Current Progress of their Polymer Composites*; Berber, M.R., Hafez, I.H., Eds.; InTech: London, UK, 2016.
7. Hayashi, T.; Endo, M. Carbon nanotubes as structural material and their application in composites. *Compos. Part B* **2011**, *42*, 2151–2157. [[CrossRef](#)]
8. Zhang, Q.; Huang, J.-Q.; Qian, W.-Z.; Zhang, Y.-Y.; Wei, F. The Road for Nanomaterials Industry: A Review of Carbon Nanotube Production, Post-Treatment, and Bulk Applications for Composites and Energy Storage. *Small* **2013**, *9*, 1237–1265. [[CrossRef](#)] [[PubMed](#)]
9. Khandoker, N.; Hawkins, S.C.; Ibrahim, R.; Huynh, C.P.; Deng, F. Tensile Strength of Spinnable Multiwall Carbon Nanotubes. *Procedia Eng.* **2011**, *10*, 2572–2578. [[CrossRef](#)]
10. Liu, Z.; Cong, W.; Kim, H.; Ning, F.; Jiang, Q.; Li, T.; Zhang, H.C.; Zhou, Y. Feasibility Exploration of Superalloys for AISI 4140 Steel Repairing using Laser Engineered Net Shaping. *Procedia Manuf.* **2017**, *10*, 912–922. [[CrossRef](#)]
11. Collins, F.; Lambert, J.; Duan, W.H. The influences of admixtures on the dispersion, workability, and strength of carbon nanotube-OPC paste mixtures. *Cem. Concr. Compos.* **2012**, *34*, 201–207. [[CrossRef](#)]
12. Siddique, R.; Mehta, A. Effect of carbon nanotubes on properties of cement mortars. *Constr. Build. Mater.* **2014**, *50*, 116–129. [[CrossRef](#)]

13. Gillani, S.S.; Khitab, A.; Ahmad, S.; Khushnood, R.A.; Ferro, G.A.; Kazmi, S.M.; Qureshi, L.A.; Restuccia, L. Improving the mechanical performance of cement composites by carbon nanotubes addition. *Procedia Struct. Integr.* **2017**, *3*, 11–17. [CrossRef]
14. Shah, S.P.; Hou, P.; Cheng, X. Durability of Cement-Based Materials and Nano-particles: A Review. In *Nanotechnology in Construction*; Sobolev, K., Shah, S.P., Eds.; Springer International Publishing: Switzerland, 2015; pp. 15–24. Available online: https://link.springer.com/chapter/10.1007/978-3-319-17088-6_2 (accessed on 27 August 2017).
15. Li, W.-W.; Ji, W.-M.; Liu, Y.; Xing, F.; Liu, Y.-K. Damping Property of a Cement-Based Material Containing Carbon Nanotube. *J. Nanomater.* **2015**, *2015*, 1–7. [CrossRef]
16. Sáez de Ibarra, Y.; Gaitero, J.J.; Erkizia, E.; Campillo, I. Atomic force microscopy and nanoindentation of cement pastes with nanotube dispersions. *Phys. Stat. Solidi A* **2006**, *203*, 1076–1081. [CrossRef]
17. Cui, H.; Yang, S.; Memon, S. Development of Carbon Nanotube Modified Cement Paste with Microencapsulated Phase-Change Material for Structural–Functional Integrated Application. *Int. J. Mol. Sci.* **2015**, *16*, 8027–8039. [CrossRef] [PubMed]
18. Arash, B.; Wang, Q.; Varadan, V.K. Mechanical properties of carbon nanotube/polymer composites. *Sci. Rep.* **2015**, *4*. [CrossRef] [PubMed]
19. Ma, J.; Larsen, R.M. Comparative Study on Dispersion and Interfacial Properties of Single Walled Carbon Nanotube/Polymer Composites Using Hansen Solubility Parameters. *ACS Appl. Mater. Interfaces* **2013**, *5*, 1287–1293. [CrossRef] [PubMed]
20. Gaffney, A.M.; Santos-Martinez, M.J.; Satti, A.; Major, T.C.; Wynne, K.J.; Gun'ko, Y.K.; Annich, G.M.; Elia, G.; Radomski, M.W. Blood biocompatibility of surface-bound multi-walled carbon nanotubes. *Nanomed. Nanotechnol. Biol. Med.* **2015**, *11*, 39–46. [CrossRef] [PubMed]
21. Lischner, J.; Arias, T.A. Material limitations of carbon-nanotube inertial balances: Possibility of intrinsic yoctogram mass resolution at room temperature. *Phys. Rev. B* **2010**, *81*. [CrossRef]
22. Li, G.Y.; Wang, P.M.; Zhao, X. Pressure-sensitive properties and microstructure of carbon nanotube reinforced cement composites. *Cem. Concr. Compos.* **2007**, *29*, 377–382. [CrossRef]
23. Luo, J.; Duan, Z.; Li, H. The influence of surfactants on the processing of multi-walled carbon nanotubes in reinforced cement matrix composites. *Phys. Stat. Solidi A* **2009**, *206*. [CrossRef]
24. Shah, S.P.; Konsta-Gdoutos, M.S.; Metaxa, Z.S.; Mondal, P. Nanoscale Modification of Cementitious Materials. In *Nanotechnology in Construction 3*; Bittnar, Z., Bartos, P.J.M., Němeček, J., Šmilauer, V., Zeman, J., Eds.; Springer: Berlin/Heidelberg, Germany, 2009; pp. 125–130.
25. Vaisman, L.; Wagner, H.D.; Marom, G. The role of surfactants in dispersion of carbon nanotubes. *Adv. Colloid Interface Sci.* **2006**, *128–130*, 37–46. [CrossRef] [PubMed]
26. Sobolkina, A.; Mechtcherine, V.; Khavrus, V.; Maier, D.; Mende, M.; Ritschel, M.; Leonhardt, A. Dispersion of carbon nanotubes and its influence on the mechanical properties of the cement matrix. *Cem. Concr. Compos.* **2012**, *34*, 1104–1113. [CrossRef]
27. Chen, Z.; Lim, J.L.G.L.; Yang, E.-H. Ultra high performance cement-based composites incorporating low dosage of plasma synthesized carbon nanotubes. *Mater. Des.* **2016**, *108*, 479–487. [CrossRef]
28. Poorgholami-Bejarpasi, N.; Sohrabi, B. Role of surfactant structure in aqueous dispersions of carbon nanotubes. *Fluid Phase Equilib.* **2015**, *394*, 19–28. [CrossRef]
29. Ghazatloo, A.; Rashidi, A.M.; Shariaty-Niasar, M. Effects of surface modification on the dispersion and thermal conductivity of CNT/water nanofluids. *Int. Commun. Heat Mass Transf.* **2014**, *54*, 1–7. [CrossRef]
30. Korayem, A.H.; Barati, M.R.; Chen, S.J.; Simon, G.P.; Zhao, X.L.; Duan, W.H. Optimizing the degree of carbon nanotube dispersion in a solvent for producing reinforced epoxy matrices. *Powder Technol.* **2015**, *284*, 541–550. [CrossRef]
31. Ferreira, F.V.; Francisco, W.; de Menezes, B.R.; Cividanis, L.D.; dos Reis Coutinho, A.; Thim, G.P. Carbon nanotube functionalized with dodecylamine for the effective dispersion in solvents. *Appl. Surf. Sci.* **2015**, *357*, 2154–2159. [CrossRef]
32. Li, Y.; Huang, X. Dispersion evaluation, processing and tensile properties of carbon nanotubes-modified epoxy composites prepared by high pressure homogenization. *Compos. Part Appl. Sci. Manuf.* **2015**, *78*, 166–173. [CrossRef]

33. D'Alessandro, A.; Rallini, M.; Ubertini, F.; Materazzi, A.L.; Kenny, J.M. Investigations on scalable fabrication procedures for self-sensing carbon nanotube cement-matrix composites for SHM applications. *Cem. Concr. Compos.* **2016**, *65*, 200–213. [[CrossRef](#)]
34. Konsta-Gdoutos, M.S.; Metaxa, Z.S.; Shah, S.P. Highly dispersed carbon nanotube reinforced cement based materials. *Cem. Concr. Res.* **2010**, *40*, 1052–1059. [[CrossRef](#)]
35. Krause, B.; Mende, M.; Pötschke, P.; Petzold, G. Dispersability and particle size distribution of CNTs in an aqueous surfactant dispersion as a function of ultrasonic treatment time. *Carbon* **2010**, *48*, 2746–2754. [[CrossRef](#)]
36. Xu, S.; Liu, J.; Li, Q. Mechanical properties and microstructure of multi-walled carbon nanotube-reinforced cement paste. *Constr. Build. Mater.* **2015**, *76*, 16–23. [[CrossRef](#)]
37. Stephens, C.; Brown, L.; Sanchez, F. Quantification of the re-agglomeration of carbon nanofiber aqueous dispersion in cement pastes and effect on the early age flexural response. *Carbon* **2016**, *107*, 482–500. [[CrossRef](#)]
38. Chaipanich, A.; Nochaiya, T.; Wongkeo, W.; Torkittikul, P. Compressive strength and microstructure of carbon nanotubes–fly ash cement composites. *Mater. Sci. Eng. A* **2010**, *527*, 1063–1067. [[CrossRef](#)]
39. Nochaiya, T.; Chaipanich, A. Behavior of multi-walled carbon nanotubes on the porosity and microstructure of cement-based materials. *Appl. Surf. Sci.* **2011**, *257*, 1941–1945. [[CrossRef](#)]
40. Metaxa, Z.S.; Seo, J.-W.T.; Konsta-Gdoutos, M.S.; Hersam, M.C.; Shah, S.P. Highly concentrated carbon nanotube admixture for nano-fiber reinforced cementitious materials. *Cem. Concr. Compos.* **2012**, *34*, 612–617. [[CrossRef](#)]
41. Morsy, M.S.; Alsayed, S.H.; Aqel, M. Hybrid effect of carbon nanotube and nano-clay on physico-mechanical properties of cement mortar. *Constr. Build. Mater.* **2011**, *25*, 145–149. [[CrossRef](#)]
42. Li, G.Y.; Wang, P.M.; Zhao, X. Mechanical behavior and microstructure of cement composites incorporating surface-treated multi-walled carbon nanotubes. *Carbon* **2005**, *43*, 1239–1245. [[CrossRef](#)]
43. Horszczaruk, E.; Mijowska, E.; Kalenczuk, R.J.; Aleksandrak, M.; Mijowska, S. Nanocomposite of cement/graphene oxide—Impact on hydration kinetics and Young's modulus. *Constr. Build. Mater.* **2015**, *78*, 234–242. [[CrossRef](#)]
44. García-Lodeiro, I.; Fernández-Jiménez, A.; Blanco, M.T.; Palomo, A. FTIR study of the sol–gel synthesis of cementitious gels: C–S–H and N–A–S–H. *J. Sol-Gel Sci. Technol.* **2008**, *45*, 63–72. [[CrossRef](#)]



© 2017 by the authors. Licensee MDPI, Basel, Switzerland. This article is an open access article distributed under the terms and conditions of the Creative Commons Attribution (CC BY) license (<http://creativecommons.org/licenses/by/4.0/>).